Supporting Information

The mechanisms of surface passivation during galena leaching by hydrogen peroxide in acetate and citrate solutions at 25–50 °C

Fatemeh Nikkhou, Fang Xia[*], Manuel Knorsch, and Artur P. Deditius

Discipline of Chemistry and Physics, College of Science, Health, Engineering and Education, Murdoch University, 90 South Street, Perth, WA 6150, Australia

*Email address: F.Xia@murdoch.edu.au

Number of pages: 9

Number of figures: 2

Number of Tables: 4

Design and Characterization techniques

Design of Experiments

The Design of Experiments (DOE) technique was employed to develop a model for determining the optimal leaching conditions.[1,2] Response surface methodology (RSM) for optimal (custom) design was used for the optimization process. Optimal design with a total number of 55 trials was applied to accommodate the adjustments to the experiments. The number of runs was chosen algorithmically to (i) ensure all possible factors combinations are included in the design; (ii) reduce the number of runs; and (iii) obtain statistically meaningful results. Four control variables were chosen, including H_2O_2 concentration (in the range of 0.21–0.84 M), type of lixiviant (2 levels, either 1 M citrate pH buffer or 1 M acetate pH buffer), particle size (5 levels including < 38 μm, 53–106 μm, 106–150 μm, 150–250 μm, and 250–355 μm), and solution pH (5 levels in the range of 3–7) (Table S1). For each trial, 80±0.1 mg galena was reacted with 1.6 mL solution at 35 °C for 6 h. After running the 55 trials (chosen randomly using the DOE method), Analysis of Variance (ANOVA) was conducted on the extraction results. DESIGN EXPERT 11.1.2.0 (DX11) program (State-Ease Inc., Minneapolis, MN, USA) was used for ANOVA analysis. By default, the optimal design includes five lack-of-fit and five replicates to estimate the error, respectively. Five sets of replicates include (Runs 22 and 49), (Runs 4 and 5), (Runs 10 and 26), (Runs 3 and 23), (Runs 7 and 51), chosen randomly by the DESIGN EXPERT software. A natural logarithm function was used to convert the experimentally obtained values to coded values used in the ANOVA analyses.

Table S1. Control values and their corresponding levels in the leaching experiments.

Control factor	Type of factor	Levels				
		1	2	3	4	5
A: H_2O_2 concentration (M)	Numerical*	(-1) to (+1)				
B: Lixiviant type	Categorical	Citrate buffer	Acetate buffer	—	—	—
C: Particle size (μm)	Categorical	< 38	53–106	106–150	150–250	250–355
D: pH	Categorical	3	4	5	6	7

*The condition is defined at two levels; (-1) and (+1); (-1) = 0.21 M H_2O_2, (+1) = 0.84 M H_2O_2. Any designed level is linearly interpolated between these two values.

Powder X-ray diffraction (PXRD)

The PXRD patterns of the solid phase after leaching were collected by a GBC Enhanced Multi-Material Analyser (EMMA), with a nickel filtered Cu Kα radiation (λ=1.5419 Å). The diverging, receiving, and scattering slits were chosen as 2°, 0.3°, and 3°, respectively. Quartz (SiO_2) was used as an internal standard. In a typical measurement, the solid residues were ground for more than 10 minutes using a pair of agate mortar and pestle to provide fine powders with an average particle size of less than 3 μm. The ground sample was mixed with the quartz standard and loaded in the middle of a zero-background sample holder. The diffraction patterns were collected over the 2-theta range of 5–70° with the scan speed of 1°·min⁻¹ and a step size of 0.02°. 'Match!' (Version: 3.6.0.111), along with the Crystallography Open Database (COD) software,[3] was used for the phase identification. Rietveld-based quantitative phase analyses of the diffraction patterns were conducted using TOPAS Academic v6.0 software. In each analysis, the background and peak shape was refined using a fifth-order polynomial function and empirical models (which uses a pseudo-Voigt function and considers both Gaussian and Lorentzian contributions), respectively. Crystallite size function was used to account for peak width broadening. The initial structural models were taken from the COD database: # 96-900-8695 for galena,[4] #96-901-1363 for sulfur,[5] and #96-900-4485 for anglesite.[6] After getting good refinement, as indicated by low values of the weighted-profile R-value R_{wp} and goodness of fit χ^2,[7] the weight percentage of each phase were calculated using the following formula,[8]

$$W_p = (SZMV)_P / \sum_i (SZMV)_i \qquad (1)$$

where W_p is the relative abundance of phase p in the leached residue, S the scale factor, Z the number of formula units per unit cell, M the molar mass of the formula unit, and V is the volume of the unit cell; i represents an individual phase in the mixture. The absolute mass was obtained by multiplying the weight percent of each phase by the mass of accurately weighed leached residue.

The internal standard method was employed for the leached residues in which some unknown peaks were observed in the low 2-theta angles (~7.2 °). A known amount of quartz standard was added in the XRD sample. The unknown peaks were excluded in the

Rietveld analysis. The determined relative quantity of each phase by the Rietveld analysis was rescaled based on the true quartz percentage. The percentage of the unknown phase was then determined by mass balance calculations.

Scanning electron microscopy (SEM) and energy dispersive spectroscopy (EDS)

Scanning EM and EDS analyses were conducted using a Zeiss 1555 VP-FESEM. To examine the surface morphology of the leached residue, representative grains were fixed on an aluminum stub using double-sided sticky copper tape. To study the cross sections of the residues, the grains were embedded in low-shrinkage epoxy resins and ground with 1200 grit abrasive papers, and finally polished by 9 μm, 3 μm, and 1 μm diamond paste. The samples were platinum-coated with a thickness of 5–10 nm for better conductivity under the electron beam. Platinum has Lα peak at 9.441 keV and Mα peak at 2.048 keV, which does not have any interference with studied elements here. Accelerating voltage of 15 kV or 20 kV was applied for SEM imaging to provide the optimum contrast and resolution. The acquisition time for EDS spectra was 60 seconds in all measurements.

Raman spectroscopy

Confocal Raman microscopy was performed on fresh galena and leached residue. The samples were fixed on aluminum stubs, and the measurements were carried out using a WITec Alpha300 RA+ confocal Raman microscope. Samples were probed using a 532 nm laser source focused on the sample with 100× objective lens with a numerical aperture of 0.9. The full Raman spectra were acquired using a camera with a thermoelectrically cooled, back-illuminated CCD chip. The first-order Raman peak of Si on a Si-wafer (520 cm^{-1}) was used for instrument calibration, and laser power was adjusted to 1 mW prior to analysis to ensure no laser-induced oxidation of the sample. Measurements were made as spot analysis with the accumulation of twenty to eighty spectra and an integration time of 0.05 to 0.1 s. The area sampled has a diameter of around 1 μm, and the spectral range was between 0 and 1020 cm^{-1}.

Electron probe micro-analysis (EPMA)

The chemical composition of the starting galena was determined using a JEOL JXA8530F microprobe equipped with five wavelength dispersive spectrometers (WDS). The accelerating voltage of 20 kV, beam current of 40 nA, and take-off angle of 40° was used for the analyses. The following crystals and spectral lines were utilized for the elemental analysis: PETJ for S Kα, Sn Lα, Ag Lα, Si Kα, Hg Mα, and Cd Lα, PETH for Sb Lα, Bi Mα, Pb Mα, LiF for Fe Kα, Cu Kα, Ni Kα, Co Kα, Zn Kα, Mn Kα, Te Lα and TAP for As Lα and Se Lα. The range of detection limits varied from 0.006 wt.% for Si to 0.078 wt.% for Hg. The method provided by Donovan and Tingle (1996) was used for the correction of mean atomic number (MAN).[9] The intensities of unknown and standard samples were corrected for dead time, and matrix correction was conducted using the ZAF algorithm.[10] The measurements were also corrected for on-peak interference.[11]

Inductively coupled plasma optical emission spectroscopy (ICP-OES)

An iCAP 7000 series ICP-OES spectrometer was employed to determine Pb concentration in the leachate. Lead concentration was measured in a radial view with a wavelength of 220.353 nm. The instrument was calibrated using six Pb standard solutions in the concentration range of 20 ppm to 250 ppm. The sample solutions were first filtered by syringe filters (pore size of 0.22 μm) and then diluted by a factor of 100 to 200 times to bring the concentration to the range of the calibration curve. In all analyses, a 0.2% nitric acid solution was used as the blank, a yttrium solution of 1 ppm was used as the internal, and the 150 ppm Pb standard solution was used as the middle range standard for quality control. Three times repetitions of each measurement resulted in a standard deviation of ±3%, confirming the accuracy and reproducibility of the analyses.

Thermodynamic analysis

The speciation diagrams for the leaching of galena in acetate and citrate solutions in the presence of H_2O_2 were constructed using the MEDUSA software.[12] The thermodynamic modeling was conducted based on the algorithm recommended by Eriksson (1979), through which Gibb's free energy is minimized, and equilibrium is assumed between all components.[13] Eh-pH diagrams were plotted using the Geochemist's Workbench (GWB) software package (v.12) with the database "thermo.com.V8.R6+.tdat".

Results of Design of Experiments (DOE)

The experimental conditions and Pb extractions of the 55 leaching experiments are summarized in Table S2. The last two columns of the table show the experimental Pb extraction versus predicted Pb extraction. The statistical significance of the leaching parameters was analyzed. The results of the ANOVA analysis are presented in Table S3. The factor (studied experimental condition such as lixiviant type) is regarded as more significant if the p-value is low or the F-value is high. Generally, p-values less than 0.05 mean that the model is significant within the 95% confidence interval.[14, 15] The p-value for the Pb extraction response model is less than 0.0001 (Table S3), suggesting that the model was significant, and there was only a 0.01% chance that F-value this large could occur due to the noise. From the p-values and F-values shown in Table S3, H_2O_2 concentration (A-H_2O_2 concentration), type of lixiviant (B-Type of Lixiviant), particle size (C-Particle size), and solution pH (D- Solution pH) are all significant parameters in galena leaching. Based on the F-values, the type of lixiviant is the most significant, followed by solution pH, H_2O_2 concentration, and particle size.

Table S2. Randomized experimental runs designed using the DOE method and the Pb extraction results.

Run	Lixiviant type	H_2O_2, M	pH	Particle size, μm	Experimental Pb extraction, %	Predicted Pb extraction, %
1	acetate	0.21	3	53−106	29.1	32.8
2	citrate	0.39	6	less than 38	68.0	72.2
3	acetate	0.52	5	250−355	40.0	45.2
4	acetate	0.52	4	250−355	51.4	51.4
5	acetate	0.52	4	250−355	51.1	51.4
6	citrate	0.34	3	250−355	3.5	3.3
7	acetate	0.55	6	150−250	24.9	22.0
8	acetate	0.53	6	106−150	28.5	30.9
9	acetate	0.73	6	250−355	21.6	22.4
10	acetate	0.43	4	106−150	19.4	21.3
11	citrate	0.21	4	150−250	3.7	3.6
12	citrate	0.65	3	53−106	3.0	2.67
13	acetate	0.26	7	150−250	4.3	5.0
14	acetate	0.79	7	less than 38	17.3	17.3
15	acetate	0.61	4	150−250	55.1	56.3
16	acetate	0.65	6	53−106	29.7	30.3
17	acetate	0.84	5	150−250	49.2	52.5
18	acetate	0.21	7	250−355	3.3	3.1
19	citrate	0.21	6	53−106	44.9	44.3
20	acetate	0.27	6	250−355	22.1	20.5
21	citrate	0.67	4	less than 38	11.5	11.6
22	citrate	0.52	5	53−106	18.6	21.8
23	acetate	0.52	5	250−355	49.7	45.2
24	citrate	0.72	6	106−150	88.1	81.5
25	citrate	0.84	7	53−106	80.2	90.0
26	acetate	0.43	4	106−150	23.5	21.3
27	citrate	0.21	5	250−355	5.6	6.4
28	citrate	0.64	5	106−150	12.9	14.4
29	acetate	0.21	4	less than 38	51.3	50.9
30	citrate	0.84	5	250−355	12.5	10.8
31	citrate	0.24	7	less than 38	45.8	45.6
32	citrate	0.73	3	150−250	4.9	6.2
33	acetate	0.21	5	106−150	40.0	35.5
34	citrate	0.55	7	106−150	59.3	59.2
35	citrate	0.81	6	250−355	66.1	68.7
36	acetate	0.55	3	150−250	43.9	34.8
37	citrate	0.68	7	250−355	53.9	55.7
38	acetate	0.35	3	53−106	25.3	22.7
39	citrate	0.84	3	less than 38	11.4	11.5

40	acetate	0.84	4	53–106	29.2	27.9
41	citrate	0.84	4	106–150	11.8	11.7
42	acetate	0.70	5	less than 38	75.1	78.3
43	citrate	0.44	4	53–106	9.5	9.8
44	acetate	0.81	3	106–150	46.6	43.4
45	acetate	0.34	3	106–150	12.1	13.5
46	citrate	0.21	3	less than 38	7.9	7.6
47	citrate	0.79	7	150–250	77.2	66.7
48	citrate	0.24	3	106–150	0.8	0.8
49	citrate	0.52	5	53–106	25.5	21.78
50	acetate	0.59	3	less than 38	57.0	58.0
51	acetate	0.55	6	150–250	19.2	22.0
52	citrate	0.42	5	150–250	12.3	11.5
53	citrate	0.53	5	less than 38	25.3	24.3
54	acetate	0.84	3	250–355	22.2	23.6
55	acetate	0.84	6	less than 38	23.3	21.8

Table S3. Results of the analysis of variance for Pb extraction.

Source	Sum of squares	DF	Mean Square	F Value	p-Value
Model	55.80	44	1.27	27.67	< 0.0001
A-H_2O_2 concentration	1.90	1	1.90	41.46	< 0.0001
B-Type of Lixiviant	9.49	1	9.49	206.97	< 0.0001
C-Particle size	3.84	4	0.9601	20.95	< 0.0001
D-Solution pH	7.71	4	1.93	42.08	< 0.0001
Residual	0.4583	10	0.0458		
Lack-of-fit	0.3339	5	0.0668	2.68	0.1513
Pure Error	0.1244	5	0.0249		
Cor Total	56.26	54			

The parameter "lack-of-fit" measures how well the model fits the data. The desirable value for the lack-of-fit is P>0.1. The calculated p-value of 0.1513 implies that the lack-of-fit parameter is not significant, and the model fits the data. The residual sum of squares (SS) is the sum of the squared difference between the actual and predicted response variable (extracted Pb). A small value of SS (0.4583) indicates that the model fits very well with the results of Pb extraction. Mean square is calculated by dividing SS by degree of freedom (df), and the lower value of mean square (0.0458 in this study) corresponds to the higher accuracy of the prediction due to a relatively good match between the actual and predicted results.

A model was developed to work out the most optimal condition for maximizing Pb extraction. Based on the statistical calculations, the developed model was the best for maximizing Pb extraction (the response variable, in this study) in the studied range of parameters. Figure S1 displays the predicted data against the experimental data for Pb extraction. From the correlation coefficient (R^2) of 0.98 between the predicted and experimental data, it is inferred that the developed model is suitable for proposed leaching conditions and Pb extraction.
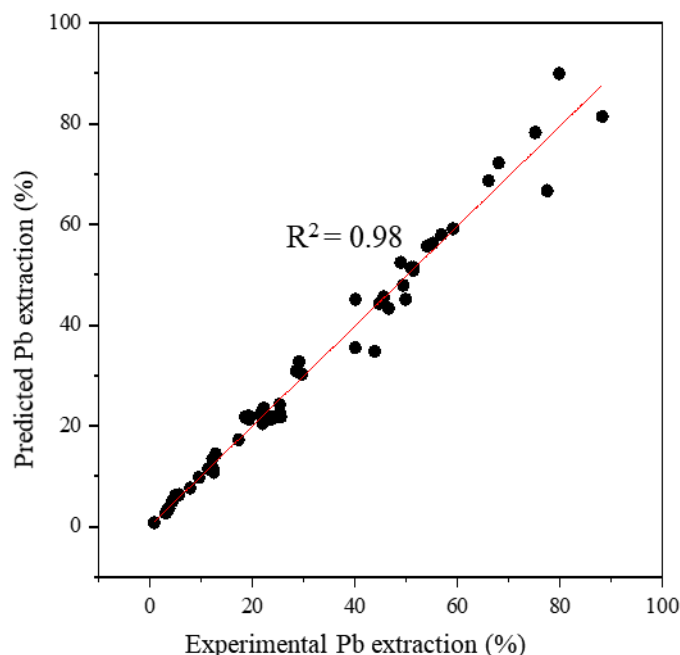
Figure S1. Predicted vs. experimental Pb extractions.

The results of the level average analysis are summarized in Figure S2, which shows the effect of the investigated factors/parameters such as H_2O_2 concentration, type of lixiviant, particle size, and solution pH on the Pb extraction variable. The red circles denote the optimal level for each factor to obtain the highest Pb extraction (Figure S2). The numerical factors (e.g., H_2O_2 concentration) change from (-1) to (+1), which is equivalent to 0.21 M and 0.84 M H_2O_2, respectively. Accordingly, any coded value from the software (which is a number between -1 and +1) is linearly interpolated and provides the actual value of the molarity. In this study, the optimum coded value of 0.85 corresponds to the actual value of 0.79 M (Figure S2a). The other control factors, including the type of lixiviant, particle size, and solution pH, were considered as the categorical factors with 2, 5, and 5 levels, respectively (Figure S2 b-d). For example, a red circle in Figure S2b at level one demonstrates that the optimum condition is level 1 of type of lixiviant, which corresponds to the citrate buffer according to Table 1. Figure S2e displays the data for Pb extraction as the response variable. The extraction results of 55 runs varied from 0.8% to 88%, depending on the experimental conditions (Table S2). The desired range of Pb extraction for optimization was considered to be in the range of 95–100%. It was observed that the optimum condition for maximizing Pb extraction to 100% is 0.79 M H_2O_2, citrate buffer (level 1), solution pH 7 (level 5), and the particle size of below 38 µm (level 1).
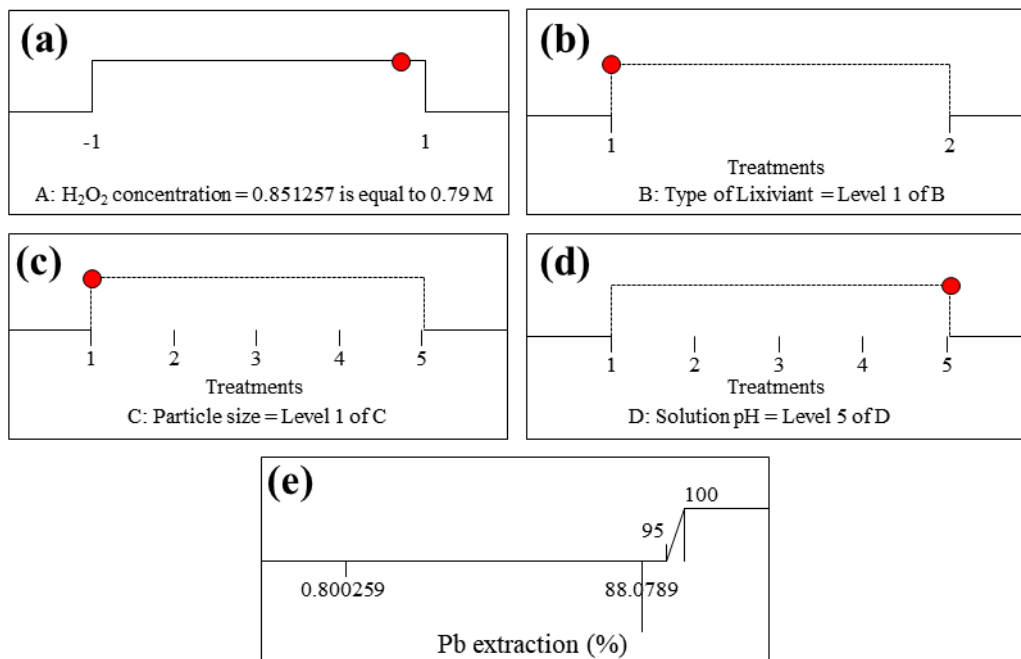
Figure S2. Optimum conditions of experimental factors for maximizing Pb extraction.

Raman results of the leached residues formed during acetate-based and citrate-based leaching

Table S4. Summary of Raman data for leached residues formed during the leaching of galena (values in cm^{-1}).

Pb-O grains	Leached galena surface - citrate solution pH 7	Sulfur precipitates	Leached galena surface - acetate solution pH 4	Assignment of peaks
82–85	82–85			Pb-O[16]
		83	82–84	S$_8$[17]
		88		S$_8$[17]
92–96	92–97			Pb-O[18]
			95–98	PbSO$_4$[19]
133–141	133–182*			Pb-O[16, 19]
			133–135	PbSO$_4$[19]
		153–154	152–154	S$_8$[17]
180–183				Pb-O[20]
		186–187		S$_8$[17]
		219	219	S$_8$[17]
		246–248		S$_8$[17]
269–278				Pb-O[16]
				S$_8$[17]
		438	438–439	PbSO$_4$ & S$_8$[19]
			449–450	PbSO$_4$[19]
		472–473	472–473	S$_8$[17]
			605–607	PbSO$_4$[19]
			639–642	PbSO$_4$[19]
964–970				nPbO * PbSO$_4$[21]
			977	PbSO$_4$[19]

* represents bulging pattern without distinct peaks

References

(1) Fisher, R. A., The Design of Experiments (Hafner). *New York* 1935, 1-27.

(2) Cochran, W. G.; Cox, G. M., *Experimental Designs: 2nd Edition.* J. Wiley: 1957; p 135.

(3) Gražulis, S.; Chateigner, D.; Downs, R. T.; Yokochi, A.; Quirós, M.; Lutterotti, L.; Manakova, E.; Butkus, J.; Moeck, P.; Le Bail, A., Crystallography Open Database–an open-access collection of crystal structures. *J. Appl. Cryst.* 2009, 42, (4), 726-729.

(4) Margulieux, G. W.; Weidemann, N.; Lacy, D. C.; Moore, C. E.; Rheingold, A. L.; Figueroa, J. S., Isocyano analogues of $[Co(CO)_4]^n$: a tetraisocyanide of cobalt isolated in three states of charge. *J. Am. Chem. Soc.* 2010, 132, (14), 5033-5035.

(5) Rettig, S.; Trotter, J., Refinement of the structure of orthorhombic sulfur, α-S_8. *Acta Cryst. Sec. C* 1987, 43, (12), 2260-2262.

(6) Jacobsen, S. D.; Smyth, J. R.; Swope, R. J.; Downs, R. T., Rigid-body character of the SO_4 groups in celestine, anglesite and barite. *Can. Mineral.* 1998, 36, 1053-1060.

(7) McCusker, L.; Von Dreele, R.; Cox, D.; Louër, D.; Scardi, P., Rietveld refinement guidelines. *J. Appl. Crystallogr.* 1999, 32, (1), 36-50.

(8) Hill, R.; Howard, C., Quantitative phase analysis from neutron powder diffraction data using the Rietveld method. *J.Appl. Crystallogr.* 1987, 20, (6), 467-474.

(9) Donovan, J. J.; Tingle, T. N., An improved mean atomic number background correction for quantitative microanalysis. *Microsc. Microanal.* 1996, 2, (1), 1-7.

(10) Armstrong, J., Quantitative analysis of silicate and oxide materials: comparison of monte carlo, ZAF, and ψ (ρz) procedures. *Microbeam Anal.* 1988, 239-246.

(11) Donovan, J. J.; Snyder, D. A.; Rivers, M. L., An improved interference correction for trace element analysis. *Microbeam Anal. (N. Y.)* 1992, 2, 23-28.

(12) Puigdomenech, I., Make equilibrium diagrams using sophisticated algorithms (MEDUSA). *Inorganic Chemistry* 2004.

(13) Eriksson, G., An algorithm for the computation of aqueous multi-component, multiphase equilibria. *Anal. Chim. Acta* 1979, 112, (4), 375-383.

(14) Dehghan, R.; Noaparast, M.; Kolahdoozan, M.; Mousavi, S., Statistical evaluation and optimization of factors affecting the leaching performance of a sphalerite concentrate. *Int. J. Miner. Process.* 2008, 89, (1-4), 9-16.

(15) Anderson, M. J.; Whitcomb, P. J., *DOE simplified: practical tools for effective experimentation.* Productivity press: 2016.

(16) Burgio, L.; Clark, R. J.; Firth, S., Raman spectroscopy as a means for the identification of plattnerite (PbO_2), of lead pigments and of their degradation products. *Analyst* 2001, 126, (2), 222-227.

(17) Nims, C.; Cron, B.; Wetherington, M.; Macalady, J.; Cosmidis, J., Low frequency Raman spectroscopy for micron-scale and in vivo characterization of elemental sulfur in microbial samples. *Sci. Rep.* 2019, 9, (1), 1-12.

(18) Wiechert, D. U.; Grabowski, S. P.; Simon, M., Raman spectroscopic investigation of evaporated PbO layers. *Thin Solid Films* 2005, 484, (1-2), 73-82.

(19) Burgio, L.; Clark, R. J., Library of FT-Raman spectra of pigments, minerals, pigment media and varnishes, and supplement to existing library of Raman spectra of pigments with visible excitation. *Spectrochim. Acta A: Mol. Biomol. Spectrosc.* 2001, 57, (7), 1491-1521.

(20) Trettenhahn, G.; Nauer, G.; Neckel, A., Vibrational spectroscopy on the PbO-$PbSO_4$ system and some related compounds: part 1. Fundamentals, infrared and Raman spectroscopy. *Vib. Spectrosc.* 1993, 5, (1), 85-100.

(21) Shapter, J. G.; Brooker, M.; Skinner, W. M., Observation of the oxidation of galena using Raman spectroscopy. *Int. J. Miner. Process.* 2000, 60, (3-4), 199-211.